

Redox-Induced Coordination Isomerization of a Phosphiobenzophospholide

Dietrich Gudat,^{*,[a]} Burhanshah Lewall,^[a] Martin Nieger,^[a] Ilka Detmer,^[a] László Szarvas,^[a] Pauli Saarenketo,^[b] and Guido Marconi^[c]

Abstract: 1-Triphenylphosphiobenzophospholide **1** reacts with $[M(\text{CO})_5\text{Br}]$ ($M = \text{Mn}, \text{Re}$) and $[\text{Mn}(\text{CO})_3(\text{naphthalene})][\text{BF}_4]$ to give complexes *cis*- $[\text{M}(\text{CO})_4(\mathbf{1})\text{Br}]$ (**5a,b**) and $[\text{Mn}(\text{CO})_3(\mathbf{1})][\text{BF}_4]$ (**6a**), respectively, featuring $\eta^1(\text{P})$ - and $\eta^5(\pi)$ -coordination of the phosphole ring. The corresponding reactions with $[\text{M}_2(\text{CO})_{10}]$ proceed with conservation of the metal–metal bond and yield, depending on the reaction temperature, dinuclear complexes $[\text{M}_2(\text{CO})_8(\mathbf{1})]$ ($M = \text{Mn}, \mathbf{7a}$) or $[\text{M}_2(\text{CO})_6(\mathbf{1})_2]$ ($M = \text{Mn}, \text{Re}, \mathbf{8a,b}$) with μ_2 -bridging $\eta^1(\text{P}):\eta^2(\text{P}=\text{C})$ coordination of the phosphole moiety. All complexes formed were characterized by spectroscopic data; **5b**, **6a**, and **8a,b** were

characterized by X-ray diffraction studies as well. The structural and ^{31}P NMR data of the dinuclear manganese complex **8a** suggest that the interaction between the metal atoms and the η^2 -bound $\text{P}=\text{C}$ double bond moieties is dominated by the $\text{L} \rightarrow \text{M}$ charge-transfer contribution; this hints at a very low back-donation ability of the central $\text{M}_2(\text{CO})_6$ fragment. Investigation of the reactions of the Mn complexes **6a** and **8a** with Mg or ferrocenium hexafluorophosphate ($[\text{Fc}][\text{PF}_6]$), respectively, revealed that the chemically reversible

mutual interconversion between both species was feasible. Likewise, oxidation of the rhenium complex **8b** with $[\text{Fc}][\text{PF}_6]$ gave spectroscopic evidence for the formation of a Re analogue of **6a**. Electrochemical studies suggested that the oxidation **8a** \rightarrow **26a** involves two consecutive single-electron-transfer steps, the first of which is electrochemically reversible and produces a metastable radical cation that is detectable by ESR spectroscopy. The mutual interconversion between **6a** and **8a** represents the first case of a reversible coordination isomerization of a phospharene that is triggered by a redox process and might stimulate further studies directed at the use of dinuclear phospharene complexes in redox-catalysis.

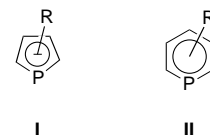
Keywords: bridging ligands • coordination modes • oxidation • phosphorus heterocycles • reduction

Introduction

Phosphorus-containing aromatic heterocycles, such as phospholyl anions (phospholides) **I** and phosphinines (phospha-benzenes) **II**, are well known for their ability to form a large variety of transition metal complexes.^[1] The exploration of the chemistry of these complexes has not only continued to attract considerable interest during the last decades,^[1] but became even more intense when it was recently shown that these species may be used as highly active and selective catalysts in

different reactions.^[1d,2] The success of aromatic phosphorus heterocycles as ligands in catalysis is, in the first place, due to their peculiar electronic properties: phospharenes are generally both weaker σ -donors and stronger π -acceptors towards transition metals in low oxidation states than, for example, tertiary phosphanes^[1,2] and thus meet the special demands for ligands in important processes like hydroformylation.

In addition to their unique electronic properties, phospharenes are distinguished by a remarkable ability to behave as ambidentate ligands that bind to transition metals in different bonding situations. Depending on the number and electron demand of the metal atoms, coordination may occur through the phosphorus lone pair or/and the π -electrons, and a variety of different coordination modes are known in which a monocyclic phospharene may donate between two and eight electrons (Scheme 1).^[1] A particularly appealing aspect, beside the number of possible bonding situations, is their potential to undergo transformations between different



[a] Prof. Dr. D. Gudat, Dr. B. Lewall, Dr. M. Nieger, I. Detmer, Dr. L. Szarvas

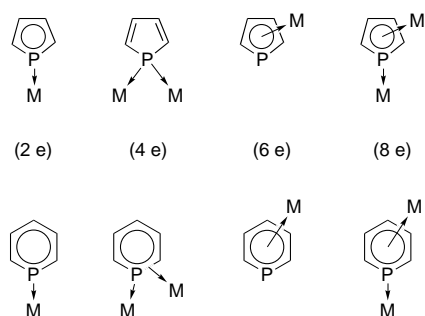
Institut für Anorganische Chemie, Universität Bonn
Gerhard-Domagk-Strasse 1, 53121 Bonn (Germany)
Fax: (+49) 228-73-53-27
E-mail: dgudat@uni-bonn.de

[b] P. Saarenketo

Department of Chemistry, University of Jyväskylä
P.O. Box 35, 40351 Jyväskylä (Finland)

[c] Dott. G. Marconi

Institut für Anorganische Chemie, Universität Erlangen-Nürnberg
Egerlandstrasse 1, 91058 Erlangen (Germany)

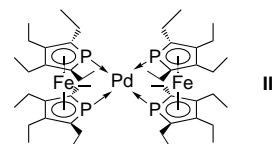


Scheme 1. Coordination modes of monocyclic phosphoarenes. The electron counting scheme implies considering the phosphinine as a neutral and the phospholide as an anionic ligand.

coordination modes. Such conversions may either proceed irreversibly, such as the long-known $\eta^1(\text{P})$ - to $\eta^6(\pi)$ -coordination isomerization of phosphinines,^[3] or even reversibly, as was recently established for the dimerization of a 1,2,4-triphospholyl nickel complex whose mechanism involves a σ - π rearrangement of the phosphoarene ligand.^[4]

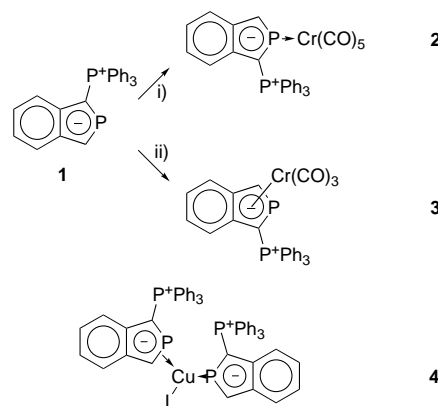
Abstract in German: 1-Triphenylphosphonio-benzo[*c*]phospholid **1** reagiert mit $[\text{M}(\text{CO})_5\text{Br}]$ ($\text{M} = \text{Mn}, \text{Re}$) und $[\text{Mn}(\text{CO})_3(\text{naphthalen})][\text{BF}_4]$ zu den Komplexen $\text{cis-}[\text{M}(\text{CO})_4(\mathbf{1})\text{Br}]$ (**5a,b**) bzw. $[\text{Mn}(\text{CO})_3(\mathbf{1})][\text{BF}_4]$ (**6a**[BF_4]) mit $\eta^1(\text{P})$ - und $\eta^5(\pi)$ -Koordinat ion des Phosphol-Rings. Die entsprechenden Reaktionen mit $[\text{M}_2(\text{CO})_{10}]$ verlaufen unter Erhalt der Metall–Metall-Bindung und liefern je nach Reaktionstemperatur entweder die dinuklearen Komplexe $[\text{M}_2(\text{CO})_8(\mathbf{1})]$ ($\text{M} = \text{Mn}$, **7a**) oder $[\text{M}_2(\text{CO})_6(\mathbf{1})_2]$ ($\text{M} = \text{Mn}, \text{Re}$, **8a,b**) mit μ_2 -verbrückender $\eta^1(\text{P})$: $\eta^2(\text{P}=\text{C})$ -Koordinat ion der Phosphol-Einheit. Alle gebildeten Komplexe wurden durch spektroskopische Daten und **5b**, **6a**[BF_4] und **8a,b** zusätzlich durch Röntgendiffraktometrie charakterisiert. Die Struktur- und ^{31}P NMR Daten des dinuklearen Mangankomplexes **8a** legen nahe, dass die Wechselwirkung zwischen den Metallatomen und der η^2 -gebundenen $\text{P}=\text{C}$ Doppelbindungseinheit durch den $\text{L} \rightarrow \text{M}$ charge-transfer Beitrag dominiert wird und sprechen damit für eine sehr niedrige Rückbindungskapazität des zentralen $\text{M}_2(\text{CO})_6$ -Fragments. Untersuchung der Reaktionen der Mn-Komplexe **6a** und **8a** mit Mg bzw. Ferrocenium Hexafluorophosphat ($[\text{Fc}][\text{PF}_6]$) belegt die Möglichkeit einer chemisch reversiblen gegenseitigen Umwandlung zwischen beiden Spezies. Entsprechend wurden bei der Oxidation des Rheniumkomplexes **8b** mit $[\text{Fc}][\text{PF}_6]$ spektroskopische Anhaltspunkte für die Bildung eines Re-Analogs von **6a** erhalten. Elektrochemische Studien ergaben Hinweise, dass die Oxidation **8a** \rightarrow **26a** in zwei konsekutiven Schritten unter Übertragung je eines Elektrons verläuft. Der erste Schritt ist elektrochemisch reversibel und liefert ein metastabiles, durch ESR-Spektroskopie nachweisbares Radikalkation. Die wechselseitige Umwandlung zwischen **6a** und **8a** ist das erste Beispiel einer reversiblen, durch einen Redox-Prozess getriggerten Koordinationsisomerisierung eines Phosphoarens und sollte weitere Untersuchungen mit dem Ziel der Nutzung dinuklearer Phosphoarene-Komplexe in der Redoxkatalyse stimulieren.

The ability to undergo reversible coordination isomerization is an important issue that may further enhance the value of a ligand for use in synthesis or catalysis. Catalytic transformations—in particular those involving consecutive oxidative addition/reductive elimination steps—frequently require that a coordinatively and electronically unsaturated complex formed as intermediate must be stabilized by a spectator ligand without permanently blocking the active site. One possible solution to this problem is the use of hemilabile ligands^[5] that exhibit both a strongly Lewis basic donor functionality ensuring permanent attachment of the ligand to the metal, and a second, weakly coordinating one that allows temporary stabilization of a vacant coordination site but is easily displaced by a new substrate. Conventional phosphorus-based hemilabile ligands include tertiary phosphanes with a further labile donor site (ether, oxazoline, ketone, etc.) that may support active intermediates by temporary chelation.^[5b] A different approach to hemilabile coordination was realized in Pd complex **III**, in which an incoming ligand may displace



one of the phosphorus lone pairs and induce a switch from μ_2 -bridging to monodentate ligation of a diphosphaferrocene unit.^[6] The key to this reaction lies in the nondirectional coordination of the lone pairs which weakens the P–Pd bonds and makes the diphosphaferrocene a rather inefficient chelating ligand.

We have recently initialized a program aimed at a detailed exploration of the chemistry of phosphonio-substituted benzophospholides.^[7,8] In the course of this study we demonstrated the ability of the zwitterion **1** to bind a transition metal both through the phosphorus lone pair and the π electrons of the phospholide ring to give the complexes **2** and **3** in a similar way to the ambidentate coordination modes of phosphinines (Scheme 2).^[8] Furthermore, we have characterized the Cu^I complex **4** whose benzophospholide ligands display distinguishable $\eta^2(\pi)$ - and $\eta^1(\text{P})$ -coordination modes in the



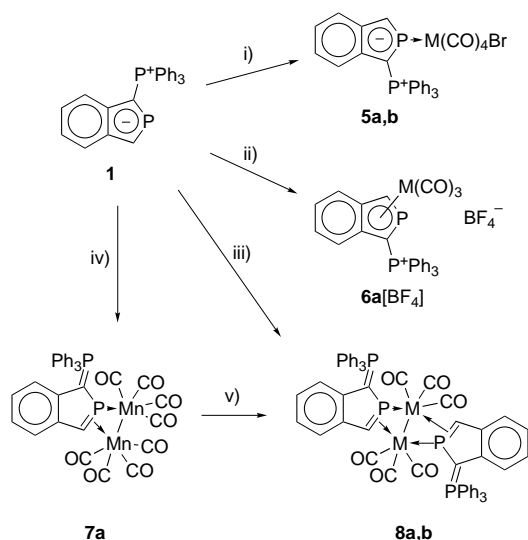
Scheme 2. i) $[\text{Cr}(\text{CO})_5(\text{cyclooctene})]$; ii) $[\text{Cr}(\text{CO})_3(\text{naphthalene})]$.

solid state, but undergo rapid dynamic exchange in solution, thus illustrating the behavior of **1** as a coordinatively mobile ligand.^[9] In this article, we report on reactions of **1** with mono- and dinuclear manganese and rhenium carbonyls whose results led to a further extension of the accessible coordination modes for **1** and to the discovery of a new reversible redox-induced coordination isomerization reaction, which is to the best of our knowledge unprecedented for phospharenes.

Results

Complex syntheses and spectroscopic studies: The metal–ligand bonding in complexes of univalent group 7 metal atoms normally differs notably from that in isoelectronic complexes of zerovalent group 6 metals due to the lower π basicity (back-donation capability) and more pronounced σ acidity of the former. In order to study the influence of these effects in complexes of phosphoniobenzophospholides, we decided to first prepare manganese and rhenium complexes of **1** that may be regarded as isoelectronic analogues of complexes **2** and **3**.

Reactions of **1** with equimolar amounts of $M(\text{CO})_5\text{Br}$ ($M = \text{Mn, Re}$) in THF proceeded with elimination of one molecule of CO to afford the $\eta^1(\text{P})$ complexes **5a,b** (Scheme 3). The



Scheme 3. $M = \text{Mn}$ (**5a, 8a**), Re (**5b, 8b**). i) 1 equiv $[\text{Mn}(\text{CO})_5\text{Br}]$ in THF at ambient temp. or 1 equiv $[\text{Re}(\text{CO})_5\text{Br}]$ in toluene, reflux; ii) 1 equiv $[\text{Mn}(\text{CO})_5(\text{naphthalene})][\text{BF}_4]$ in CH_2Cl_2 ; iii) 0.5 equivs. $[\text{M}_2(\text{CO})_{10}]$ in xylene, reflux; iv) 1 equiv $[\text{Mn}_2(\text{CO})_{10}]$ in toluene, reflux; v) xylene, reflux.

rhenium complex **5b** was isolated as a red solid after precipitation with *n*-hexane, whereas the manganese complex **5a** was obtained in crude form as an orange oil, which could not be further purified. The constitution of **5a,b** was established by NMR and IR spectroscopy and mass spectrometry. The complexes are highly air and moisture sensitive and decompose both in pure form and, more rapidly, in solution to give unidentifiable brownish-green oils.

The ^{31}P NMR spectra of **5a** and **b** exhibit the expected AX-type patterns. The coordination shift of the ring phosphorus

atom in **5a** ($\Delta\delta^{\text{coord}} = \delta(\text{complex}) - \delta(\text{ligand}) = -65$) is about twice as large as in **2** ($\Delta\delta^{\text{coord}} = -29$ ^[8]), and the signal is broadened by scalar relaxation of the second kind due to coupling with the ^{55}Mn nucleus ($I = 5/2$, 100% natural abundance); this points to a $\eta^1(\text{P})$ coordination of ligand **1**. The increase of $\Delta\delta^{\text{coord}}$ upon replacement of Mn by the heavier Re atom (**5b**: $\Delta\delta^{\text{coord}} = -105$) reproduces the known trend for phosphane– $M(\text{CO})_5$ complexes of group 6 metals.^[10] The ^{13}C and ^1H chemical shifts of the atoms in the benzophospholide units of **5a,b** are—apart from moderate coordination shifts for the carbons adjacent to the ring phosphorus atom ($\Delta\delta^{\text{coord}} \leq \pm 10$)—similar to those in free **1** or the Cr complex **2**. The *cis* arrangement of the benzophospholide and bromide ligands follows from the presence of three ^{13}C NMR signals with relative intensities of 1:1:2, attributable to CO ligands, and the observation of similar patterns in the carbonyl region of the IR spectra ($\tilde{\nu} = 2051, 2021, 2011, 1977 \text{ cm}^{-1}$ (**5a**), 2046, 2013, 2000, 1943 cm^{-1} (**5b**)) as for *cis*- $[\text{MBr}(\text{CO})_4(\text{Ph}_3\text{P})]$ ($\tilde{\nu} = 2091, 2028, 2012, 1962 \text{ cm}^{-1}$ ($M = \text{Mn}$); 2100, 2015, 1998, 1940 cm^{-1} ($M = \text{Re}$)^[11]). Three of the observed bands for **5a,b** occur at similar energies as in the Ph_3P complexes, while the bands at highest wave numbers are red shifted by some 40 cm^{-1} .

Known synthetic routes to η^5 phospholide complexes of manganese or rhenium include the thermolysis of $[\text{M}(\eta^1\text{-phospholyl})(\text{CO})_5]$ with cleavage of two CO and η^1/η^5 -coordination isomerization of the phospholyl ligand, exchange of the arene in $[\text{Mn}(\text{CO})_3(\text{arene})]^+$, and thermal reactions of phenylphospholes or bisphospholes with $\text{M}_2(\text{CO})_{10}$.^[1a,c] Attempts to induce thermal η^1/η^5 -coordination isomerization in **5a** and **b** proceeded with decomplexation of **1** and deposition of black solid materials. Clean formation of the η^5 -benzophospholide complex **6a[BF₄]** was observed, however, by treating **1** with $[\text{Mn}(\text{CO})_5(\text{naphthalene})][\text{BF}_4]$ ^[12] (Scheme 3). The choice of a noncoordinating solvent like CH_2Cl_2 proved necessary; donor solvents such as THF are known to convert the Mn–arene complex to a solvent complex (e.g. $[\text{Mn}(\text{CO})_3(\text{THF})_3]^+$) on a minute timescale,^[12] and the reaction of this intermediate with **1** proceeded rather unselectively and afforded a product mixture whose further work-up proved unfeasible. The complex **6[BF₄]** was isolated by precipitation with hexane and characterized by IR and NMR spectroscopy, FAB-MS, and an X-ray diffraction study.

The η^5 -coordination mode of the benzophospholide ring in the cation **6a** is evidenced by a large coordination shift ($\Delta\delta^{\text{coord}} = -190$), the lack of any signal broadening for the ring phosphorus atom, and by further considerable coordination shifts for the other atoms in the phosphole ring, which are most prominent for the nuclei in the adjacent CH fragment ($\Delta\delta^{\text{coord}} = -1.9$ (^1H), -32.0 (^{13}C)). Similar features have been observed for the chromium complex **3**.^[8] The carbonyl region of the IR spectrum of **6a[BF₄]** shows the expected three-band pattern ($\tilde{\nu} = 2040, 1972, 1922 \text{ cm}^{-1}$). The band at highest energy (a_1 mode) displays a slight blue shift compared with both $[\text{CpMn}(\text{CO})_3]$ ($\tilde{\nu} = 2025 \text{ cm}^{-1}$ ^[13]) and $[(\eta^5\text{-3,4-Me}_2\text{C}_4\text{H}_2\text{P})\text{Mn}(\text{CO})_3]$ ($\tilde{\nu} = 2032 \text{ cm}^{-1}$ ^[14]).

The reactions of the benzophospholide **1** with $\text{M}_2(\text{CO})_{10}$ ($M = \text{Mn, Re}$) in refluxing xylene do not proceed, as in the case of phenylphospholes or bisphospholes, with metal–metal bond cleavage to give η^5 -phospholyl complexes.^[1a,c] Rather

they lead to the formation of the dinuclear complexes **8a,b** featuring two μ_2 -bridging phosphoniobenzophospholides in a rare $\eta^1(\text{P}):\eta^2(\text{P}=\text{C})$ coordination mode (Scheme 3). Specific incorporation of only a single benzophospholide was observed when the reaction was conducted at lower temperature in refluxing toluene. The complex formed, **7a**, was shown to be a precursor to **8a**; it can be successfully converted into the latter upon reaction with an excess of **1** in refluxing xylene. The complexes **7a** and **8a,b** precipitated from the reaction mixtures and were isolated after recrystallization from THF/hexane as medium to dark red, moderately air-sensitive crystalline solids. All products were insoluble in hexane and only moderately soluble in toluene, but dissolved readily in THF. They were characterized by microanalyses, FAB-mass spectrometry, and IR and NMR spectroscopy. The constitution of the dinuclear complexes **8a,b** was further proven by means of X-ray diffraction studies.

The ^{31}P NMR spectra of **7a** and **8a,b** have a single AX-type pattern. The signals attributable to the ring phosphorus atoms in the manganese complexes are distinguished by small coordination shifts ($\Delta\delta^{\text{coord}} = -2.0$ (**7**), -7.6 (**8a**)) and line broadenings due to interaction with the quadrupolar ^{55}Mn nuclei; this indicates $\eta^1(\text{P})$ coordination of **1**. The corresponding signal of the rhenium complex **8b** appears as a sharp doublet with a larger coordination shift ($\Delta\delta^{\text{coord}} = -90.5$). The ^1H and ^{13}C spectra of **7a** and **8a** exhibit marked negative coordination shifts for the nuclei in the CH moiety adjacent to the ring phosphorus atom [$\Delta\delta^{\text{coord}}(^1\text{H}) = -3.64$ (**7a**), -4.01 (**8a**), $\Delta\delta^{\text{coord}}(^{13}\text{C}) = -23.3$ (**7a**), -22.5 (**8a**)], whereas the corresponding changes for the Ph_3P -substituted carbon atom are much smaller [$\Delta\delta^{\text{coord}}(^{13}\text{C}) = -11.6$ (**7a**), -3.6 (**8a**)]. Three ^{13}C NMR signals attributable to CO ligands for **8a** and a three-band pattern in the carbonyl region of the IR spectra of **8a** ($\tilde{\nu} = 1997, 1963, 1913\text{ cm}^{-1}$) and **8b** ($\tilde{\nu} = 2008, 1976, 1913\text{ cm}^{-1}$) suggest that both molecules have symmetric molecular structures with equivalent $\text{M}(\text{CO})_3$ fragments. The IR spectrum of **7a** had a more complicated pattern; this suggests a less symmetric molecular structure.

Even if the observed ^1H and ^{13}C NMR data appeared to be in accord with the molecular structures presented in Scheme 3, and the suggested constitutions of **8a,b** were verified by X-ray diffraction studies, the unique low values of $\Delta\delta^{\text{coord}}(^{31}\text{P})$ for **7a** and **8a** seemed at a first glance to be incompatible with the presence of a π -bound $\text{P}=\text{C}$ double bond moiety. In order to check for the possible presence of different coordination modes in solution and the solid state, which has precedence in the chemistry of phosphalkenes,^[15] a ^{31}P MAS spectrum of **8a** was recorded. However, the observed similarity of the isotropic chemical shifts ($\delta^{31}\text{P}^{\text{iso}} = 184$ (br) for the *endo*- and $14.4/16.4$ ppm for the exocyclic phosphorus atoms) to the solution values suggested that the molecular structures in solution and solid phase are identical. The origin of the unusual chemical shift of the ring phosphorus atom will be discussed later.

Crystal-structure studies: Single crystals of **5b**, **6a**[BF_4], **8a**· 3THF , and **8b**· $\text{THF}\cdot 0.25\text{hexane}$ suitable for X-ray diffraction studies were grown by slow cooling of solutions in THF/*n*-hexane or CH_2Cl_2 /*n*-hexane. Thermal ellipsoid plots of the

molecular structures of **5b**, **6a**[BF_4], and **8a** are displayed in Figures 1–3, below, and selected bond data for all compounds are listed in Table 1. The crystals of **8b** (not shown) contain two crystallographically independent molecules per asymmetric unit whose molecular structures do not differ significantly from each other or from that of **8a**.

Table 1. Relevant bond lengths [pm] in the complexes **5b**, **6**[BF_4], and **8a,b**. The two halves of the molecules of **8a,b** are crystallographically nonequivalent, and the crystal structure of **8b** contains further two crystallographically independent molecules in the asymmetric unit.

	5b	6 [BF_4]	8a	8b	
P1–C2	175.0(3)	179.49(16)	175.1(4)	174.5(7)	175.8(7)
			175.2(4)	176.6(7)	175.3(6)
P1–C9	169.9(3)	174.79(19)	175.3(4)	177.1(7)	175.4(7)
			175.0(4)	175.7(7)	174.6(7)
C2–C3	144.2(4)	145.3(2)	146.5(5)	147.6(9)	146.2(9)
			146.7(5)	145.7(9)	147.0(9)
C3–C8	144.1(4)	143.4(2)	143.1(5)	141.5(9)	143.5(9)
			141.3(6)	143.2(10)	142.4(9)
C8–C9	141.3(5)	142.5(3)	144.3(5)	145.8(9)	146.1(9)
			145.4(6)	146.0(10)	145.6(9)
C2–P2	174.7(3)	178.05(16)	173.8(4)	173.5(7)	172.8(7)
			173.3(4)	173.1(7)	172.7(7)
P1–M	246.64(8)	236.81(5)	223.56(11)	237.72(17)	237.74(17)
			223.49(11)	237.82(17)	237.57(16)
P1–M'			244.76(11)	260.09(18)	261.53(17)
			241.62(11)	262.73(17)	263.00(18)
C2–M		214.71(16)			
C3–M		222.63(16)			
C8–M		223.20(17)			
C9–M	–	217.36(17)	228.9(4)	238.6(7)	239.1(6)
			226.4(4)	238.6(6)	238.9(6)
M–M'			281.78(8)	300.68(4)	299.41(4)
M–C1A	200.3(4)	180.90(19)	180.2(4)	192.8(8)	192.7(8)
			180.2(4)	192.5(7)	193.9(8)
M–C1B	204.0(5)	179.0(2)	180.3(4)	193.9(7)	190.3(7)
			178.7(4)	192.9(7)	194.4(8)
M–C1C	193.3(4)	182.42(19)	179.3(5)	193.8(8)	192.7(7)
			180.5(4)	192.5(8)	193.0(8)
M–C1D	195.9(4)				
M–Br	262.72(4)				

The ring system of the $\eta^1(\text{P})$ -coordinated phosphoniobenzophospholide in **5b** (Figure 1) is essentially planar. The exocyclic P2–C2 bond (174.7(3) pm) is longer and the

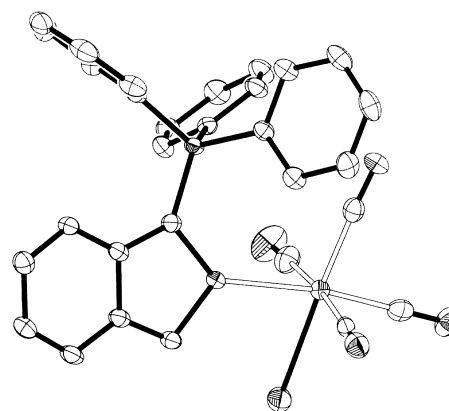


Figure 1. ORTEP plot showing the molecular structure of **5b** in the crystal; thermal ellipsoids are at the 50% probability level, H atoms are omitted for clarity. Selected bond lengths and angles are given in Table 1.

endocyclic P1–C2 (175.0(3) pm) and P1–C9 bonds (169.9(3) pm) are shorter than in free **1** (P2–C2 172.55(11), P1–C2 176.62(11), P1–C9 171.71(14) pm^[16]) and resemble the corresponding bonds in the chromium complex **2** (P2–C2 174.4(1), P1–C2 176.7(2), P1–C9 169.1(2) pm^[7a]). The remaining intraligand bond lengths are identical in all three compounds within experimental accuracy. The distorted trigonal planar geometry at the P1 atom of **5b** (sum of bond angles 358°) is characterized by a marked difference between the two C2–P1–Re1 (138.09(11)°) and C9–P1–Re1 (125.07(12)°) bond angles, which is presumably due to steric interference between the Ph₃P moiety and the ancillary ligands at the rhenium atom. The Re1–P1 (246.64(8) pm) and Re–C lengths in **5b** (Re1–C1A 200.3(4), Re1–C1B 204.0(5), Re1–C1C 193.3(4), Re1–C1D 195.9(4) pm) are close to the corresponding bond lengths in *cis*-[ReX(CO)₄(PPh₂H)] [X = Cl, I; P–Re 245.9–246.2 pm, Re–C 191.7–192.0 (*trans* to X), 193.0–195.9 (*trans* to PPh₂H), 198.1–200.7 pm (*trans* to CO)^[17]] and display a similar increase in M–C bond lengths upon change of the *trans*-ligand from halide to phosphane and CO.

The molecular structure of **6a**[BF₄] (Figure 2) consists of discrete anions and cations that display a similar tripodal geometry to the chromium complex **3**.^[8] The intraligand bond

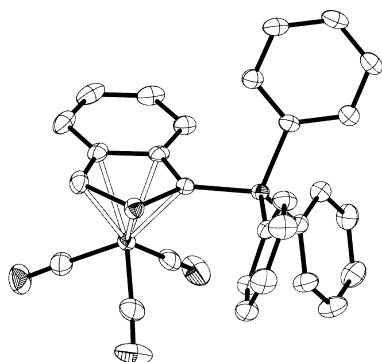


Figure 2. ORTEP plot showing the molecular structure of the cation **6a** in the crystal; thermal ellipsoids are at the 50% probability level, H atoms are omitted for clarity. Selected bond lengths and angles are given in Table 1.

lengths and angles in **6a** and **3** are—apart from the elongation of the exocyclic P2–C2 bond (178.05(16) in **6a** vs. 175.5(2) pm in **3**^[8])—indistinguishable within experimental error. The Mn–P1 (236.81(5) pm) and Mn–C bond lengths (214.7–223.2 pm) in the phosphole ring as well as the M–C lengths to carbon atoms of CO ligands (179.0–182.4 pm) in **6a** fit in with the corresponding values for phosphacymantrenes (Mn–P 237–238 pm, Mn–C(ring) 215–222 pm, Mn–C(CO) 178–183 pm^[14]). The distance between the metal and the center of the π -

coordinated ring (178.8(1) pm) matches that in cyclopentadienyls of Mn (177.4 ± 2.1 pm^[18]) and Cr (178.8 ± 2.0 pm^[18]), but is considerably shorter than that in **3** (187.7(1) pm^[8]). Comparison of individual M–C bond lengths reveals, as in the case of **3**, closer contacts to the C2/C9 atoms (average length 216 pm) than to the C3/C8 atoms (average length 223 pm), even though the deviation is less pronounced than for **3** (223 vs. 233 pm^[8]).

The molecular structures of **8a** (Figure 3) and **8b** contain discrete dinuclear complexes with slightly shorter M–M bond lengths (**8a**: 281.78(8) pm, **8b**: 299.41(4)/300.68(4) pm) than in the corresponding dicarbonyls (Mn₂(CO)₁₀: 290.38(6) pm, Re₂(CO)₁₀: 304.1(1) pm^[20]); this confirms that the M–M bonds have remained intact. Each metal is surrounded by three facially arranged carbonyls, the phosphorus lone pair of one, and the P1–C9 double bond of a second benzophospholide unit. Each benzophospholide thus bridges both metal atoms in a μ_2 -(η^1 (P): η^2 (P=C)) fashion, and both ligands have a *cis* orientation with respect to the M₂(CO)₆ core and are arranged in such a way that the planes of the two fused ring systems are nearly orthogonal and the bulky Ph₃P moieties point away from each other.

Looking more closely at the bonding situation of the phosphorus heterocycles, the mean values of the P1–M bonds (**8a**: 223.5(1) pm for M = Mn; **8b**: 237.7(1) pm for M = Re) defining the “end-on” phosphorus–metal interactions are in the lower range of the lengths in arylphosphane complexes of these metals (Mn–P 2.23–2.44, mean 2.30 pm; Re–P 2.27–2.63, mean 2.43 pm); the Mn–P bond lengths fall into the range found for [η^5 -C₅R₅)Mn(PAr₃)(L)₂] (Mn–P 222–230 pm^[21]) but are longer than that in [CpMn(CO)₂P(μ -NR)₂Re(CO)₄] (212.3 pm^[22]) with a η^1 (P)-bound aminoiminophosphane. The P1–Mn and C9–M lengths (average 243.2 and 227.6 pm, respectively) in **8a** are close to the upper limit of known bond lengths in π -phospholyl and phosphalkene complexes of manganese (P–Mn 232.6–243.8, mean 236.8(5) pm; C–Mn 212.5–225.0, mean 218.3(5) pm^[21]) while the P1–Re bonds in **8b** (average 261.9 pm) are longer than and the C9–Re bonds (average 238.8 pm) similar to the corresponding ones in the only comparable complex,

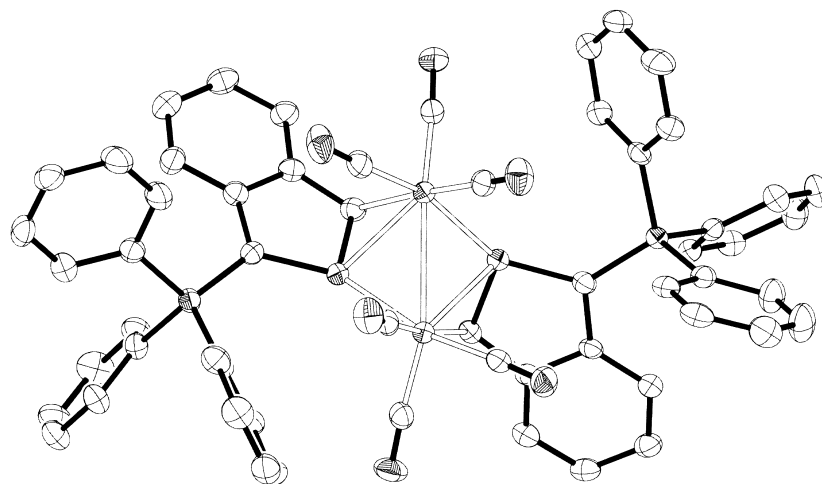


Figure 3. ORTEP plot showing the molecular structure of **8a** in the crystal; thermal ellipsoids are at the 50% probability level, H atoms are omitted for clarity. Selected bond lengths and angles are given in Table 1.

$[\text{Re}(\eta^5\text{-tBu}_2\text{C}_2\text{P}_3)(\text{CO})_3]$ (P–Re 253.5–255.5 pm, P–C 239.5 pm^[23]). Presumably, these distortions, as well as the fact that the metal atoms do not lie exactly above the edge of the η^2 -coordinated five-membered ring but are shifted outwards, are due to the geometric constraints associated with the bridging coordination mode.

The π -coordinated P1–C9 bonds (average 175.2 (**8a**), 175.7 pm (**8b**)) are longer than the corresponding bonds in the η^1 -bound ligand in **5b** (169.9 pm) or free **1** (171.71(14) pm^[16]), but still much shorter than those in π -bound phosphalkenes (mean 182.8 pm^[21]), or in other known complexes with η^2 - $\pi(\text{P}=\text{C})$ -bound phosphoniobenzophospholides (1.794–1.830 pm^[7e, f]). The sum of intraligand bond angles at the C9 atom in **8a** of 353(6)° (including those involving the H9 atom whose position was located and freely refined) indicates a much lower degree of pyramidalization compared with values of 320–330° in previously known $\eta^2(\text{P}=\text{C})$ -complexes of phosphonio-benzophospholides or phosphalkenes.^[7f, 21]

Oxidation/reduction reactions: Comparison of the composition of the complexes **6a** and **8a** reveals that two equivalents of **6a** only differ from **8a** by two electrons. Given the great flexibility of the ligand **1** toward different coordination modes, it seemed likely that mutual transformations between the complexes by redox reactions should be feasible.

In accord with this hypothesis it was found that ferrocenium hexafluorophosphate ($[\text{Fc}][\text{PF}_6]$, 2 equivs) reacted with **8a** in THF with an immediate color change from deep red to orange. The ³¹P NMR spectrum of the reaction mixture confirmed that quantitative conversion into the cation **6a** had occurred. When the rhenium complex **8b** was allowed to react under identical conditions, ³¹P NMR spectroscopy likewise disclosed the formation of a main product whose data (AX spin system, $\delta^{31}\text{P} = 26.4, 23.8$; $J_{\text{PP}} = 53.2$ Hz) are in accord with the presence of a corresponding rhenium π -complex $[\text{Re}(\eta^5\text{-1})(\text{CO})_3]^+$, **6b**. Unfortunately, separation of this product from the by-products formed and further characterization was unfeasible.

The reverse conversion of the cationic manganese π complex **6a** into the neutral dimer **8a** proved possible by treating the former with activated magnesium.^[24] As before, the reaction was signaled by an immediate color change from orange to deep red, and quantitative formation of the desired product was verified by means of ³¹P NMR spectroscopy.

In order to unveil further mechanistic details, the electrochemical reduction/oxidation of the complexes **6a** and **8a,b** was further studied by cyclic voltammetry. The cation **6a** was found to undergo both irreversible electrochemical oxidation at an anodic peak potential $E_{\text{pa}} = 1150$ mV, and irreversible reduction at a cathodic peak potential of $E_{\text{pc}} = -1010$ mV. Reversing the potential after the reduction step resulted in the appearance of a new pair of oxidation/reduction waves at a standard potential $E_{1/2}(\text{d}I/\text{d}E) = 363$ mV (Figure 4a,b); this indicated that a new electrochemically active reaction product had formed. The ratio between the cathodic and anodic peak currents ($I_{\text{pc}}/I_{\text{pa}} = 1.02$) and the peak separation ($\Delta E_{\text{p}} = 75$ mV) match the expected values for an electrochemically reversible reaction.

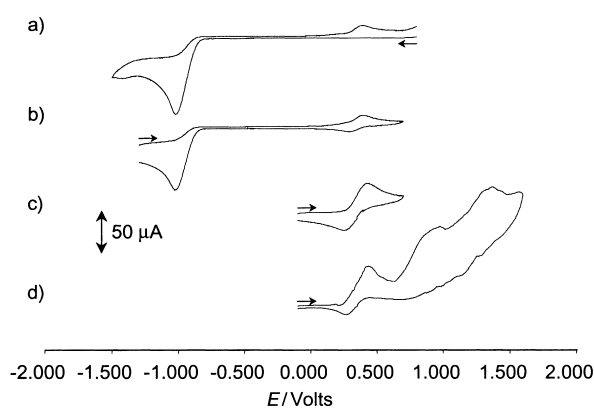


Figure 4. Cyclic voltammograms (in $\text{CH}_2\text{Cl}_2/0.1\text{M}$ Bu_4NBF_4 , scan rate 100 mV s^{-1} , potentials vs. SCE) of **6a** and **8a** with different potential ranges and start potentials. a) Scan reversal after the irreversible reduction of **6a** produces a new oxidation wave; this indicates the formation of a new electrochemically active species. b) A cyclic voltammogram obtained with pre-reduction of **6a** reveals this oxidation process to be reversible. c) The first oxidation of **8a** appears reversible if the oxidative scan is halted at 700 mV. d) Scanning **8a** to higher potentials produces further irreversible oxidation waves; the decrease in intensity of the return wave corresponding to the first oxidation step indicates the onset of further oxidation of the intermediate formed.

The dinuclear complex **8a** undergoes a first, electrochemically reversible oxidation at a standard potential $E_{1/2}(\text{d}I/\text{d}E) = 340$ mV and further irreversible oxidation processes at higher potentials (Figure 4c,d). The reversible redox process is the same as that observed for **6a** but without the necessary preceding reduction step; this suggests that **8a** is the product of the irreversible electrochemical reduction of the cation **6a**. The return wave following the oxidation step is quenched completely if the potential is scanned above values of 2.2 V; this indicates exhaustive irreversible oxidation of the initially formed species under these conditions. The electrochemical oxidation of the rhenium complex **8b** occurred at a similar potential ($E_{\text{pa}} = 417$ mV) to that of **8a** but was not reversible. A similar behavior of corresponding rhenium and manganese derivatives had previously been observed by Mathey et al. in electrochemical studies on phospholyl complexes.^[25]

Summarizing the results of the electrochemical studies suggests that the oxidation of **8a** to **6a** involves two consecutive one-electron steps. The first step is electrochemically reversible and should thus produce a radical intermediate that is stable on the timescale of the experiment, while the second step is immediately followed by a subsequent chemical reaction. Experimental proof for the existence of a radical intermediate was obtained by the observation of a transient ESR signal ($g = 2.05$) during the oxidation of **6a** with a substoichiometric amount of $[\text{Fc}][\text{PF}_6]$ at -60°C in the cavity of an ESR spectrometer. Further characterization of the radical was prevented, however, by the lack of any hyperfine structure.

Discussion

Metal–ligand bonding interactions: The pattern of Re–C bond lengths in the $\eta^1(\text{P})$ -complex **5b** suggests that the π -

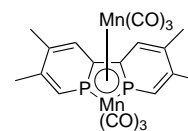
acceptor properties of the ligand **1** roughly match those of tertiary phosphanes. This interpretation is on the whole in accord with the IR data^[26] and matches the conclusion drawn from previous studies on chromium and nickel complexes of **1**.^[8] The rather short Re–P bond length is considered to reflect the small covalency radius of the formally sp₂-hybridized phosphorus atom rather than a high covalent bond order; this is well in accord with the low Lewis basicity of **1** and the low back-donation capability of the Re^I fragment, and fits in with the observed low thermal stability of the complexes **5a,b**.

The distribution of M–C and M–P bond lengths and the pronounced P–C bond lengthening upon π coordination in the η^5 complex **6a** are in accord with computational results that showed that the phosphorus and the adjacent carbon atoms of phosphoniobenzophospholides have the largest coefficients in both the HOMO and LUMO and should thus exhibit the strongest donor/acceptor interaction with a metal atom.^[16] The shorter M–C/M–P bond lengths and the less pronounced tendency toward a “slipped” coordination of the phosphole ring (as expressed by the smaller deviation between C2/9 vs. C3/8 lengths) in **6a** compared with the Cr complex **3** point to a strengthening of the metal–ligand π -bonding interactions in the former. Based on the found lengths, the bonding situation in **6a** should thus be similar to that in phosphacymantrenes. Considering, however, that Mathey et al. interpreted a blue-shift of the ν CO bands in (phospha)cymantrenes as an indication of a weaker electron-donor ability of the π -bound ligand,^[14] the IR data suggest a decrease in the net L \rightarrow M charge transfer upon going from [(Cp)Mn(CO)₃] to [$(\eta^5$ -Me₂C₄H₂P)Mn(CO)₃] and finally to the cation **6a**. Even though this trend appears at first glance to contradict the conclusions drawn from the structure correlation, a common explanation might be found if shifts in covalent L \rightarrow M and L \rightarrow M charge transfer and purely electrostatic contributions are separately accounted for. A further analysis of these factors requires additional computational studies, which are outside the scope of this work.

Adopting the description of the complexes **7a** and **8a,b** as containing a metal–metal bond bridged by one (**7a**) or two benzophospholide ligands that donate two electrons to each metal, both metal atoms obey the 18e rule. The disruption of the 10 π delocalization in the η^2 (P=C)-coordinated benzophospholide ring system is not unprecedented^[7e, f, 8] and benefits without doubt from the comparatively low resonance energy in the free ligand^[16] and the possibility of stabilizing the remaining π electrons in an aryl–ylide-type bonding situation^[7e] as depicted in Scheme 3. The moderate P–C bond lengthening and the low degree of pyramidalization at the carbon atom of the π -bound P=C moiety in **8a,b** point, in terms of the Dewar–Chatt–Duncanson model, to a low degree of d(M) \rightarrow $\pi^*(L)$ charge transfer and, thus, low metallacycle character. This suggests that the coordinated double bond acts predominantly as a π donor rather than as a π acceptor. A similar bonding situation has recently been established for the copper complex **4** and in that case was shown to be associated with an unusually low ³¹P coordination shift of the phosphorus atom in the double bond moiety.^[9] Following the same arguments likewise allows the small ³¹P coordination shifts observed for **7a** and **8a** to be rationalized.

Considering that complexes with η^2 (P=C)-bound phosphoniobenzophospholides display substantial metallacycle character if the ligand is bound to the electron-rich CpCo^[7e] of the CpMo(CO)₂ fragments^[7f] leads us to suggest that the low degree of d(M) \rightarrow $\pi^*(L)$ back donation in **7a** and **8a,b** hints at a very limited π -acceptor power for the M₂(CO)₆ or M₂(CO)₈ fragments.

A topologically comparable n(P), η^2 (π) coordination of a phosphinine was also observed in the complex [Os₃(μ -H)₂(μ_3 -(η^2 -P=C(Os,Os')): η^1 -P(Os''))-PC₅H₄tBu)(CO)₉]^[27]—even though in this case the structural parameters suggest that there is a different electronic situation with a high degree of d(M) \rightarrow $\pi^*(L)$ back donation—and in complex **IV**,^[28] which was available from the reaction



IV

of the free bisphosphinine with Mn₂(CO)₁₀. Although both **8a** and **IV** feature two phosphoarene rings behaving as 8e donors to a Mn₂(CO)₆ fragment, the metrical parameters indicate a marked difference in bonding situations: whereas in **8a** the π coordination results only in a very limited perturbation of the benzophospholide π system and the Mn–Mn bond is conserved, complex **IV** is best described in terms of a Mn(CO)₃ complex of a P₂C₂Mn metallacycle that lacks a localized Mn–Mn σ bond, and in which the electron delocalization in the central metallacycle takes place at the expense of the aromaticity of the phosphinine rings.^[28]

Redox-induced coordination changes: The results of the experimental studies gave evidence that the overall reaction of **8a** to yield two molecules of **6** proceeds in two consecutive one-electron oxidation steps. With regard to the electrochemical reversibility of the first step, the intermediate formed is still considered to be a dinuclear species. Even though the ESR experiments disclosed no further structural details, it appears reasonable to assume that the initial oxidation step involves removal of one electron from the M–M bond, and that the intermediate may thus be formulated as a metal-centered radical cation with a one-electron M–M bond. In contrast to the reduction of bisphosphinine complexes, in which additional electrons are transferred to ligand-centered orbitals,^[29] the phosphoarene is in this case not directly involved in the oxidation reaction. This inert behavior is in accord with the previously reported oxidation stability of phospholyl π complexes.^[25] Mononuclear (poly)phospholyl complexes with an odd number of electrons have also been reported in the case of [(Cp*)Co(η^5 -tBu₂C₄H₄P)]^[30] and the 17e complex [(η^5 -tBu₂C₂P₃)₂Mn]^[31] in which, according to ESR and computational results, the unpaired electron occupies a metal-centered orbital.

The observation of the chemically reversible interconversion between cationic **6a** and neutral **8a** proves the stability of the phosphoarene π -electron system toward oxidation, and highlights once more the previously noticed^[8] balanced coordination behavior of the zwitterion **1**. The reversible coordination change between **6a** and **8a** is of further interest in the context of the mechanism of the reactivity of η^5/η^6 complexes of phosphoarenes. Although the generation of

these species must not necessarily be preceded by the formation of complexes featuring $\eta^1(\text{P})$ or mixed $\eta^1(\text{P})/\pi$ coordination of the phosphorus heterocycle,^[32] the interplay between compounds of both types has been proven in the case of a triphospholyl–Ni complex,^[4] and reaction sequences involving changes between $\eta^1(\text{P})$ or $\eta^1(\text{P})/\eta^2(\text{PC})$ and η^5/η^6 coordination of phospharenes may be of more general significance.

Conclusion

The studies reported have disclosed a number of Mn and Re complexes with $\eta^1(\text{P})$, $\eta^5(\pi)$, and mixed $\mu_2\text{-}\eta^1(\text{P})\text{:}\eta^2(\text{P}=\text{C})$ coordination of the ligand **1**, as well as the possibility of switching reversibly between the last two modes in redox reactions. The structural change during the coordination isomerization induces a concomitant variation in the electronic situation (change from a 4e- to 6e-donor mode), this confirms that the benzophospholide may behave as variable electron donor and shows certain characteristics of hemilabile coordination. Beside the dynamic aspects, these reactions further highlight the stability of the benzophospholide π -electron system during a process involving cleavage of a metal–metal bond in two consecutive single-electron-transfer steps. Considering that dinuclear complexes are of interest in many catalytic transformations, including redox catalysis, the findings presented here should stimulate further investigations of phosphoniobenzophospholide complexes in this area.

Experimental Section

General remarks: All manipulations were carried out under dry argon. Solvents were dried by standard procedures. Compound **1**^[6] and $[\text{Mn}(\text{CO})_5(\text{naphthalene})][\text{BF}_4]^{[2]}$ were prepared as described. Solution NMR spectra: Bruker AMX300 (^1H : 300.1 MHz, ^{31}P : 121.5 MHz, ^{13}C : 75.4 MHz); solid state NMR spectra: Varian Unity 400 (^{31}P 161.9 MHz); chemical shifts referenced to external TMS (^1H , $\delta = 100.000000$ MHz; ^{13}C , $\delta = 25.145020$ MHz), 85% H_3PO_4 (^{31}P , $\delta = 40.480747$ MHz); positive signs denote shifts to lower frequencies, and coupling constants are given as absolute values; prefixes *i*-, *o*-, *m*-, *p*- denote atoms of phenyl substituents and atoms in the benzophospholide ring are denoted as C-4, 5-H, etc; MS: VG Instruments VG 12-250; FTIR spectra: Nicolet Magna 550; elemental analyses: Heraeus CHNO-Rapid. Melting points were determined in sealed capillaries. Electrochemical measurements were conducted by using a PAR Model 173 potentiostat equipped with a PAR Model 276 interface. The cyclic voltammograms were recorded from solutions in CH_2Cl_2 containing Bu_4NBF_4 (0.1 M) as supporting electrolyte and by using a glassy carbon disk as working electrode, a coil of platinum wire as auxiliary electrode, and a saturated calomel electrode as reference electrode. Three compartment cells were used with Vycor-tips (Glassware, Inc.) separating the compartments containing reference, working, and auxiliary electrodes. The working electrode was polished with SiC powder (1000 mesh) prior to each measurement, and the apparatus was deoxygenated with a stream of argon. ESR spectra were acquired by using a Bruker ESP 300 E spectrometer (X-band).

Bromotetracarbonyl-(1-triphenylphosphoniobenzoc[phospholide- κ P)-manganese(II) (5a): A solution of $[\text{Mn}(\text{CO})_5\text{Br}]$ (0.76 mmol) and **1** (290 mg, 0.76 mol) in THF (20 mL) was stirred for 24 hours at room temperature, turning from bright yellow to deep orange. Addition of *n*-hexane (15 mL) afforded separation of a highly viscous orange oil. The solvent was decanted off, and the residue was washed with additional *n*-hexane (10 mL) and dried under vacuum. Yield: 380 mg (81%); ^1H NMR ($[\text{D}_8]\text{THF}$, 30 °C):

$\delta = 8.5$ (dd, $^2J(\text{P,H}) = 30.9$ Hz, $^4J(\text{P,H}) = 5.5$ Hz, 1H; 3-H), 7.6–8.0 (m, 16H; C_6H_5 , 7-H), 6.6–6.9 (m, 3H; 4-H–6-H); $^{13}\text{C}\{^1\text{H}\}$ NMR ($[\text{D}_8]\text{THF}$, 30 °C): $\delta = 224.7$ (br, CO), 218.0 (br, 2CO), 211.5 (br, CO), 149.0 (dd, $^1J(\text{P,C}) = 30.5$ Hz, $^3J(\text{P,C}) = 9.2$ Hz, C-3), 143.5 (dd, $^3J(\text{P,C}) = 15.6$ Hz, $^2J(\text{P,C}) = 3.8$ Hz, C-3a), 146.4 (dd, $^2J(\text{P,C}) = 6.4$ Hz, $^2J(\text{P,C}) = 11.4$ Hz, C-7a), 134.8 (d, $^2J(\text{P,C}) = 9.9$ Hz, *o*-C), 134.4 (s, *p*-C), 128.7 (dd, $^1J(\text{P,C}) = 57.6$ Hz, $^3J(\text{P,C}) = 1.0$ Hz, *i*-C), 129.9 (d, $^3J(\text{P,C}) = 12.2$ Hz (*m*-C), 120.7 (d, $^3J(\text{P,C}) = 3.6$ Hz, C-4), 119.6 (s, C-5), 120.9 (d, $^3J(\text{P,C}) = 16.4$ Hz, C-7), 120.1 (s, C-6), 85.9 (d, $^1J(\text{P,C}) = 103$ Hz, C-1); $^{31}\text{P}\{^1\text{H}\}$ NMR ($[\text{D}_8]\text{THF}$, 30 °C): $\delta = 125.2$ (br, $^2J(\text{P,P}) = 64$ Hz), 14.7 (d, $^2J(\text{P,P}) = 64$ Hz); IR (CH_2Cl_2): $\tilde{\nu} = 2051$, 2021, 2011, 1976 cm^{-1} ($\tilde{\nu}\text{CO}$); MS (FAB, mNBA): m/z (%) = 183 (100) [$\text{C}_{12}\text{H}_8\text{P}^+$]; 533 (60) [$\text{C}_{30}\text{H}_{20}\text{O}_3\text{Mn}^+$].

Bromotetracarbonyl-(1-triphenylphosphoniobenzoc[phospholide- κ P)

rhenium(II) (5b): A solution of $[\text{Re}(\text{CO})_5\text{Br}]$ (21 mg, 0.5 mmol) and **1** (200 mg, 0.5 mmol) in toluene (10 mL) was heated under reflux for 2 hours, turning gradually from yellow to orange-red. Cooling to ambient temperature and addition of *n*-hexane (10 mL) caused precipitation of a yellow-orange solid. The product was collected by filtration, washed with *n*-hexane (10 mL), and recrystallized from toluene/hexane (2:1). Yield: 280 mg (72%); m.p. 167 °C (dec.); ^1H NMR ($[\text{D}_8]\text{THF}$, 30 °C): $\delta = 8.8$ (dd, $^2J(\text{P,H}) = 27.7$ Hz, $^4J(\text{P,H}) = 1.8$ Hz, 1H; 3-H), 7.6–8.1 (m, 16H; C_6H_5 , 7-H), 6.6–6.9 (m, 3H; 4-H–6-H); $^{13}\text{C}\{^1\text{H}\}$ NMR ($[\text{D}_8]\text{THF}$, 30 °C): $\delta = 211.5$ (d, $^2J(\text{P,C}) = 11.0$ Hz, CO), 185.8 (s, CO), 183.9 (2CO), 144.7 (dd, $^2J(\text{P,C}) = 7.6$ Hz, $^2J(\text{P,C}) = 12.9$ Hz, C-7a), 143.6 (dd, $^3J(\text{P,C}) = 15.4$ Hz, $^2J(\text{P,C}) = 1.4$ Hz, C-3a), 141.8 (dd, $^1J(\text{P,C}) = 42.1$ Hz, $^3J(\text{P,C}) = 9.7$ Hz, C-3), 135.1 (d, $^2J(\text{P,C}) = 10.3$ Hz, *o*-C), 134.4 (d, $^4J(\text{P,C}) = 3.0$ Hz, *p*-C), 130.4 (d, $^3J(\text{P,C}) = 12.6$ Hz, *m*-C), 124.8 (dd, $^1J(\text{P,C}) = 90.4$ Hz, $^3J(\text{P,C}) = 1.5$ Hz, *i*-C), 122.1 (d, $^3J(\text{P,C}) = 17.1$ Hz, C-7), 121.7 (d, $^4J(\text{P,C}) = 6.1$ Hz, C-6), 121.5 (dd, $^3J(\text{P,C}) = 3.6$ Hz, $^4J(\text{P,C}) = 4.8$ Hz, C-5), 120.2 (d, $^5J(\text{P,C}) = 1.5$ Hz, C-4), 80.6 (dd, $^1J(\text{P,C}) = 107.5$ Hz, $^1J(\text{P,C}) = 9.5$ Hz, C-1); $^{31}\text{P}\{^1\text{H}\}$ NMR ($[\text{D}_8]\text{THF}$, 30 °C) $\delta = 85.4$ (d, $^2J(\text{P,P}) = 63.6$ Hz), 13.9 (d, $^2J(\text{P,P}) = 63.6$ Hz); IR (CH_2Cl_2): $\tilde{\nu} = 2046$, 2013, 2000, 1943 cm^{-1} ($\tilde{\nu}\text{CO}$).

[triacarbonyl- $\kappa^3\text{C}$ -(1-triphenylphosphoniobenzoc[phospholide- $\kappa^5\text{C}$ P)

manganese(II)] tetrafluoroborate (6a[BF₄]): A solution of $[\text{Mn}(\text{CO})_5(\text{naphthalene})][\text{BF}_4]^{[2]}$ (280 mg, 0.84 mmol) and **1** (390 mg, 0.76 mol) in CH_2Cl_2 (20 mL) was stirred for 2 hours at room temperature, turning from bright yellow to deep orange. Addition of *n*-hexane (15 mL) produced an orange-yellow precipitate, which was filtered off and washed with *n*-hexane (10 mL). Yield: 470 mg (98%); m.p. 197 °C (dec.); ^1H NMR ($[\text{D}_8]\text{THF}$, 30 °C): $\delta = 6.35$ (dd, $^2J(\text{P,H}) = 35.6$ Hz, $^4J(\text{P,H}) = 3.1$ Hz, 1H; H-3), 7.6–8.0 (m, 15H; C_6H_5), 6.7–7.5 (m, 4H; 4-H–7-H); $^{13}\text{C}\{^1\text{H}\}$ NMR ($[\text{D}_8]\text{THF}$, 30 °C): $\delta = 226.0$ (br, CO), 141.7 (dd, $^2J(\text{P,C}) = 7.0$ Hz, $^2J(\text{P,C}) = 7.2$ Hz, C-7a), 140.4 (d, $^2J(\text{P,C}) = 9.5$ Hz, *o*-C), 136.8 (d, $^3J(\text{P,C}) = 12.6$ Hz (*m*-C), 136.0 (d, $^3J(\text{P,C}) = 19.0$ Hz, C-3a), 134.3 (s, *p*-C), 134.2 (s, C-6), 127.4 (brs, C-5), 124.9 (dd, $^1J(\text{P,C}) = 89.6$ Hz, *i*-C), 124.7 (dd, $^3J(\text{P,C}) = 3.0$ Hz; $^4J(\text{P,C}) = 4.9$ Hz, C-4), 116.8 (dd, $^3J(\text{P,C}) = 11.4$ Hz, $^3J(\text{P,C}) = 5.6$ Hz, C-7), 106.3 (dd, $^1J(\text{P,C}) = 69.0$ Hz, $^3J(\text{P,C}) = 7.3$ Hz, C-3), 81.5 (dd, $^1J(\text{P,C}) = 82.8$ Hz, $^1J(\text{P,C}) = 76.8$ Hz, C-1); $^{31}\text{P}\{^1\text{H}\}$ NMR ($[\text{D}_8]\text{THF}$, 30 °C): $\delta = 29.3$ (d, $^2J(\text{P,P}) = 57.8$ Hz), 27.0 (d, $^2J(\text{P,P}) = 57.8$ Hz); IR (CH_2Cl_2): $\tilde{\nu} = 2040$, 1972, 1922 cm^{-1} ($\tilde{\nu}\text{CO}$); MS (FAB, mNBA): m/z (%) = 533 (100) [$\text{C}_{29}\text{H}_{20}\text{O}_3\text{P}_2\text{Mn}^+$]; 449 (70) [$\text{C}_2\text{H}_2\text{O}_2\text{P}_2\text{Mn}^+$].

Octacarbonyl-(μ_2 -1-triphenylphosphoniobenzoc[phospholide- κ P): $\kappa^2\text{P}$)

dimanganese-(Mn–Mn) (7a): A solution of **1** (150 mg, 0.38 mmol) and $[\text{Mn}_2(\text{CO})_{10}]$ (150 mg, 0.38 mol) in toluene (15 mL) was heated under reflux for two hours. A bright red solid precipitated from the solution and was filtered off, washed with *n*-hexane, and recrystallized from THF/*n*-hexane (5:1). Yield: 160 mg (58%); m.p. 204 °C (dec.); ^1H NMR ($[\text{D}_8]\text{THF}$, 30 °C): $\delta = 7.5$ –7.9 (m, 15H; C_6H_5), 6.95 (m, 1H; 4-H), 6.8 (m, 2H; 5/6-H), 6.65 (m, 1H; 7-H), 4.95 (dd, $^2J(\text{P,H}) = 31.8$ Hz, $^4J(\text{P,H}) = 4.25$ Hz, 1H; 3-H); $^{13}\text{C}\{^1\text{H}\}$ NMR ($[\text{D}_8]\text{THF}$, 30 °C): $\delta = 149.8$ (dd, $^3J(\text{P,C}) = 13.9$ Hz, $^2J(\text{P,C}) = 4.6$ Hz, C-3a), 145.4 (dd, $^2J(\text{P,C}) = 6.5$ Hz, $^2J(\text{P,C}) = 6.9$ Hz, C-7a), 135.0 (d, $^2J(\text{P,C}) = 10.3$ Hz, *o*-C), 133.9 (d, $^4J(\text{P,C}) = 2.9$ Hz, *p*-C), 129.8 (d, $^3J(\text{P,C}) = 12.6$ Hz (*m*-C), 124.2 (dd, $^1J(\text{P,C}) = 90.8$ Hz, $^3J(\text{P,C}) = 1.6$ Hz, *i*-C), 121.0 (d, $^3J(\text{P,C}) = 12.3$ Hz, C-7), 123 (br, C-5/6), 120 (br, C-4), 63.45 (dd, $^1J(\text{P,C}) = 113.5$ Hz, $^1J(\text{P,C}) = 13.9$ Hz C-1), 54.0 (d, $^1J(\text{P,C}) = 45.5$ Hz, C-3), signals attributable to CO ligands could not be unambiguously assigned due to severe line broadening owing to interaction with the quadrupolar ^{55}Mn nuclei; $^{31}\text{P}\{^1\text{H}\}$ NMR ($[\text{D}_8]\text{THF}$, 30 °C): $\delta = 186.9$ (br, $^2J(\text{P,P}) = 72$ Hz), 15.5 (d, $^2J(\text{P,P}) = 72.5$ Hz); IR (CH_2Cl_2): $\tilde{\nu} = 2061$, 2009, 1974, 1961, 1947, 1925 cm^{-1} ($\tilde{\nu}\text{CO}$); MS (FAB, mNBA): m/z (%) = 728 (20) [$\text{C}_{34}\text{H}_{20}\text{O}_8\text{P}_2\text{Mn}_2^+$], 533 (95) [$\text{C}_{29}\text{H}_{20}\text{O}_3\text{P}_2\text{Mn}^+$].

Hexacarbonyl-(μ_2 -1-triphenylphosphoniobenzophospholide- κ P: κ^2 PC) dimanganese (Mn–Mn) (8a**) and hexacarbonyl-(μ_2 -1-triphenylphosphoniobenzophospholide- κ P: κ^2 PC) dirhenium (Re–Re) (**8b**):** A solution of **1** (300 mg, 0.76 mmol) and $[M_2(CO)_{10}]$ (0.38 mmol, M = Mn: 150 mg, M = Re: 240 mg) in xylene (15 mL) was heated under reflux for 2 hours. The dark red crystalline precipitate formed was filtered off, washed with *n*-hexane, and recrystallized from THF/*n*-hexane (5:1).

8a: Yield: 350 mg (88%); m.p. 218 °C (dec.); 1H NMR ($[D_8]THF$, 30 °C): δ = 7.6–8.0 (m, 15H; C_6H_5), 6.6–7.6 (m, 4H; 4-H–7-H), 4.19 (dd, $^2J(P,H)$ = 28.9 Hz, $^4J(P,H)$ = 9.3 Hz, 1H; 3-H); $^{13}C\{^1H\}$ NMR ($[D_8]THF$, 30 °C): δ = 226.8 (br, CO), 225.3 (d, $^2J(P,C)$ = 5.9 Hz, CO), 224.8 (br, CO), 149.8 (dd, $^3J(P,C)$ = 13.9 Hz, $^2J(P,C)$ = 4.6 Hz, C-3a4), 145.4 (dd, $^2J(P,C)$ = 6.5 Hz, $^2J(P,C)$ = 6.9 Hz, C-7a), 135.6 (d, $^2J(P,C)$ = 9.9 Hz, *o*-C), 133.5 (s, *p*-C), 129.8 (d, $^3J(P,C)$ = 12.2 Hz (*m*-C), 126.2 (dd, $^1J(CP)$ = 90.4 Hz, *i*-C), 121.5 (br, C-4), 121.8 (d, $^3J(P,C)$ = 9.5 Hz, C-78), 120.4 (s, C-6), 118.6 (br, C-5), 63.45 (dd, $^1J(P,C)$ = 113.5 Hz, $^1J(P,C)$ = 13.9 Hz C-1), 55.5 (d, $^1J(P,C)$ = 45.5 Hz, C-3); $^{31}P\{^1H\}$ NMR ($[D_8]THF$, 30 °C): δ = 181.2 (br, $^2J(P,P)$ = 74 Hz), 14.2 (d, $^2J(P,P)$ = 74.4 Hz); IR (CH_2Cl_2): $\tilde{\nu}$ = 1997, 1963, 1913 cm^{-1} ($\bar{\nu}CO$); MS (FAB, mNBA): m/z (%) = 1067 (30) $[C_{58}H_{40}O_6P_4Mn_2]^+$, 533 (40) $[C_{29}H_{20}O_3P_2Mn]^+$; elemental analysis calcd (%) for $C_{58}H_{40}O_6P_4Mn_2$: C 65.31, H 3.78; found: C 65.04, H 4.52.

8b: Yield 390 mg (78%); m.p. 221 °C; 1H NMR ($[D_8]THF$, 30 °C): δ = 7.4–7.9 (m, 15H; C_6H_5), 6.5–7.6 (m, 4H; 4-H–7-H), 4.57 (dd, $^2J(P,H)$ = 30.3 Hz, $^4J(P,H)$ = 12.2 Hz, 1H; 3-H); $^{31}P\{^1H\}$ NMR ($[D_8]THF$, 30 °C): δ = 97.3 (d, $^2J(P,P)$ = 73.1 Hz), 13.8 (d, $^2J(P,P)$ = 73.1 Hz); IR (CH_2Cl_2): $\tilde{\nu}$ = 2008, 1976, 1913 cm^{-1} ($\bar{\nu}CO$); FAB-MS (mNBA): m/z (%) = 1329 (20) $[C_{58}H_{40}O_6Re_2]^+$, 533 (50) $[C_{29}H_{20}O_3Re]^+$; elemental analysis calcd (%) for $C_{58}H_{40}O_6P_4Re_2$: C 52.41, H 3.03; found C 51.46, H 3.13.

Crystal-structure determinations of 5b, 6a[BF₄], 8a·3 THF, and 8b·THF·0.25 hexane: The data were collected on a Nonius KappaCCD diffractometer at –150 °C with $Mo_{K\alpha}$ radiation (λ = 0.71073 Å). The structures of **6a** and **8a** were solved by direct methods and those of **5b** and **8b** by Patterson methods (SHELXS-97^[33]). The non-hydrogen atoms were refined anisotropically, H atoms were refined by using a riding model (full-matrix least-squares refinement on F^2 (SHELXL-97^[34]). Details of data collection and refinement are given in Table 2. Empirical absorption corrections from multiple reflections were applied for **5b** and **8b**.

CCDC-190421 (**5b**), 190422 (**6a**[BF₄]), 190423 (**8a**), and 190424 (**8b**) contain the supplementary crystallographic data for this paper. These data can be obtained free of charge via www.ccdc.cam.ac.uk/conts/retrieving.html (or from the Cambridge Crystallographic Data Centre, 12 Union Road, Cambridge CB2 1EZ, UK; fax: (+44) 1223-33633; or deposit@ccdc.cam.ac.uk).

Acknowledgement

This work was financially supported by the Deutsche Forschungsgemeinschaft (GK “Spektroskopie kondensierter und isolierter Moleküle”, L.S.), the Finnish Academy (P.S.), and the DAAD (M.N.). We thank Dr. W. Hoffbauer, University of Bonn, for recording the ^{31}P CP/MAS NMR spectra and Prof. Dr. U. Zenneck, University of Erlangen-Nürnberg, for helpful discussions of the ESR data.

- a) F. Mathey, *Coord. Chem. Rev.* **1994**, *137*, 1; b) P. Le Floch, F. Mathey, *Coord. Chem. Rev.* **1998**, *179–180*, 771; c) K. B. Dillon, F. Mathey, J. F. Nixon, *Phosphorus: The Carbon Copy*, Wiley, Chichester **1998**, and references therein; d) F. Mathey, *J. Organomet. Chem.* **2002**, *646*, 15; e) C. Ganter, *J. Chem. Soc. Dalton Trans.* **2001**, 3541.
- L. Weber, *Angew. Chem.* **2002**, *114*, 583; *Angew. Chem. Int. Ed.* **2002**, *41*, 563.
- a) G. Märkl in *Multiple Bonds and Low Coordination Chemistry in Phosphorus Chemistry* (Eds.: M. Regitz, O. Scherer), Thieme, Stuttgart, **1990**, pp. 220ff; b) F. Nief, C. Charrier, F. Mathey, M. Simalty, *J. Organomet. Chem.* **1980**, *187*, 277.
- F. W. Heinemann, H. Pritzkow, M. Zeller, U. Zenneck, *Organometallics* **2000**, *19*, 4283.
- a) C. S. Slone, D. A. Weinberger, C. A. Mirkin, *Prog. Inorg. Chem.* **1999**, *48*, 233; b) P. Braunstein, F. Naud, *Angew. Chem.* **2001**, *113*, 702; *Angew. Chem. Int. Ed.* **2001**, *40*, 680.
- X. Sava, L. Ricard, F. Mathey, P. Le Floch, *Organometallics* **2000**, *19*, 4899.

Table 2. Crystallographic data, structure solution and refinement of **5b**, **6a**[BF₄], **8a**·3 THF, and **8b**·THF·0.25 hexane

	5b	6a [BF ₄]	8a ·3 THF	8b ·THF·0.25 hexane
formula	C ₃₀ H ₂₀ BrO ₄ P ₂ Re	C ₂₉ H ₂₀ BF ₄ MnO ₃ P ₂	C ₅₈ H ₄₀ Mn ₂ O ₆ P ₄ –3 THF	C ₅₈ H ₄₀ O ₆ P ₄ Re ₂ –THF–0.25 hexane
M_r	772.5	620.1	1283.0	1422.9
dimensions [mm]	0.30 × 0.10 × 0.10	0.50 × 0.50 × 0.50	0.20 × 0.20 × 0.08	0.30 × 0.20 × 0.03
crystal system	monoclinic	monoclinic	monoclinic	triclinic
space group	$P2_1/c$ (No. 14)	$P2_1/n$ (No. 14)	$P2_1/c$ (No. 14)	$P\bar{1}$ (No. 2)
a [Å]	14.8334(3)	9.7337(3)	15.1785(5)	11.1870(1)
b [Å]	9.8976(2)	27.7512(6)	22.9256(6)	21.9031(2)
c [Å]	19.8558(3)	10.2818(3)	18.0850(6)	25.4990(3)
α [°]				67.201(1)
β [°]	105.124(1)	90.453(2)	101.727(2)	82.064(1)
γ [°]				81.196(1)
V [Å ³]	2814.16(9)	2777.25(13)	6161.8(3)	5670.69(10)
Z	4	4	4	4
ρ [g cm ⁻³]	1.82	1.48	1.38	1.67
μ [mm ⁻¹]	5.89	0.65	0.57	4.43
$F(000)$	1488	1256	2664	2794
T [K]	123(2)	123(2)	123(2)	123(2)
$2\theta_{max}$ [°]	56.4	50.0	50.0	50.0
	–19 ≤ h ≤ 19	–11 ≤ h ≤ 11	–18 ≤ h ≤ 18	–13 ≤ h ≤ 13
	–13 ≤ k ≤ 13	–31 ≤ k ≤ 32	–27 ≤ k ≤ 27	–26 ≤ k ≤ 26
	–24 ≤ l ≤ 25	–12 ≤ l ≤ 12	–21 ≤ l ≤ 21	–29 ≤ l ≤ 30
No. of measured data	64079	20756	47020	64726
No. of unique data	6697	4852	10512	19877
R_{int}	0.063	0.040	0.048	0.064
refinement on	F^2	F^2	F^2	F^2
No. of parameters/restraints	343/0	361/0	765/242	1370/171
R [for $I > 2\sigma(I)$]	0.028	0.028	0.057	0.041
$wR2$ (all data)	0.071	0.074	0.168	0.097
max./min. difference peak [e Å ⁻³]	–2.07/0.64	–0.30/0.49	–1.04/1.38	–2.55/1.59

- [7] a) D. Gudat, M. Schrott, M. Nieger, *Chem. Commun.* **1995**, 1541; b) D. Gudat, A. W. Holderberg, N. Korber, M. Nieger, M. Schrott, *Z. Naturforschung* **1999**, *54*, 1244; c) D. Gudat, S. Hüp, V. Bajorat, M. Nieger, *Z. Anorg. Allg. Chem.* **2001**, 627, 1119; d) S. Hüp, M. Nieger, D. Gudat, M. Betke-Hornfeck, D. Schramm, *Organometallics* **2001**, *20*, 2679; e) D. Gudat, S. Hüp, M. Nieger, *Z. Anorg. Allg. Chem.* **2001**, 627, 2269; f) D. Gudat, S. Hüp, M. Nieger, *J. Organomet. Chem.* **2002**, *643*, 181.
- [8] D. Gudat, S. Hüp, L. Szarvas, M. Nieger, *Chem. Commun.* **2000**, 1637.
- [9] D. Gudat, M. Nieger, K. Schmitz, L. Szarvas, *Chem. Commun.* **2002**, 1820.
- [10] K. R. Dixon in *Multinuclear NMR* (Ed.: J. Mason), Plenum, New York, **1987**, pp. 369ff.
- [11] a) W. Hieber, G. Faulhaber, F. Theubert, *Z. Anorg. Allg. Chem.* **1962**, *314*, 125; b) P. W. Jolly, F. G. A. Stone, *J. Chem. Soc.* **1965**, 5259.
- [12] S. Sun, L. K. Yeung, D. Sweigart, *Organometallics* **1995**, *14*, 6.
- [13] B. V. Lokshin, E. B. Rusach, V. N. Setkina, N. I. Pyshograeva, *J. Organomet. Chem.* **1974**, *77*, 69.
- [14] F. Mathey, A. Mitschler, R. Weiss, *J. Am. Chem. Soc.* **1978**, *100*, 5748.
- [15] a) T. A. van der Knaap, F. Bickelhaupt, H. van der Poel, G. van Koten, C. H. Stam, *J. Am. Chem. Soc.* **1982**, *104*, 1756; b) H. W. Kroto, S. I. Klein, M. F. Meidine, J. F. Nixon, R. K. Harris, K. J. Packer, P. Reams, *J. Organomet. Chem.* **1985**, *280*, 281.
- [16] S. Hüp, L. Szarvas, M. Nieger, D. Gudat, *Eur. J. Inorg. Chem.* **2001**, 2763.
- [17] a) T. S. A. Hor, P. M. N. Low, Y. K. Yan, L.-K. Liu, Y.-S. Wen, *J. Organomet. Chem.* **1993**, *448*, 131; b) U. Florke, H.-J. Haupt, *Z. Kristallogr.* **1990**, *192*, 290.
- [18] Results of a search of the CSD database for complexes containing the fragment $\eta^5\text{-C}_5\text{R}_5\text{M}(\text{CO})_3$ in which M = Cr, Mn.
- [19] a) L. Brunet, F. Mercier, L. Ricard, F. Mathey, *Angew. Chem.* **1994**, *106*, 812; *Angew. Chem. Int. Ed. Engl.* **1994**, *33*, 742; b) L. Brunet, F. Mercier, L. Ricard, F. Mathey, *Polyhedron* **1994**, *13*, 2555; c) B. Deschamps, L. Ricard, F. Mathey, *Organometallics* **1999**, *18*, 5688.
- [20] M. R. Churchill, K. N. Amoth, H. J. Wasserman, *Inorg. Chem.* **1981**, *20*, 1609.
- [21] Result of a request in the CSD database.
- [22] O. J. Scherer, E. Franke, J. Kaub, *Angew. Chem.* **1986**, *98*, 83; *Angew. Chem. Int. Ed. Engl.* **1986**, *25*, 96.
- [23] M. Al-Ktaifani, J. C. Green, P. B. Hitchcock, J. F. Nixon, *J. Chem. Soc. Dalton Trans.* **2001**, 1726.
- [24] "Riecke Magnesium" as described in: *Active Metals* (Ed.: A. Fürstner), Wiley-VCH, Weinheim **1996**
- [25] a) A. Breque, F. Mathey, C. Santini, *J. Organomet. Chem.* **1979**, *165*, 129; b) P. Lemoine, M. Gross, P. Braunstein, F. Mathey, B. Deschamps, J. H. Nelson, *Organometallics* **1984**, *3*, 1303.
- [26] Given the sparseness of the data available and the consideration that the observed deviation of one of carbonyl stretching frequencies between **5a,b** and *cis*-[MBr(CO)₄(Ph₃P)] (M = Mn, Re) may be both of electronic or steric origin, a concise explanation for effect is currently unfeasible.
- [27] A. J. Arce, A. J. Deeming, Y. De Sanctis, J. Manzur, *Chem. Commun.* **1993**, 325.
- [28] P. Le Floch, N. Maigrot, C. Charrier, F. Mathey, *Inorg. Chem.* **1995**, *34*, 5070.
- [29] a) S. Choua, H. Sidorenkova, T. Berclaz, M. Geoffroy, P. Rosa, N. Mézailles, L. Ricard, F. Mathey, P. Le Floch, *J. Am. Chem. Soc.* **2000**, *122*, 12227; b) P. Rosa, N. Mézailles, L. Ricard, F. Mathey, P. Le Floch, Y. Jean, *Angew. Chem.* **2001**, *113*, 1291; *Angew. Chem. Int. Ed. Engl.* **2001**, *40*, 1251.
- [30] K. Forissier, L. Ricard, D. Carmichael, F. Mathey, *Organometallics* **2000**, *19*, 954.
- [31] T. Clark, A. Elvers, F. W. Heinemann, M. Hennemann, M. Zeller, U. Zenneck, *Angew. Chem.* **2000**, *112*, 2174; *Angew. Chem. Int. Ed. Engl.* **2000**, *39*, 2087.
- [32] N. Mézailles, L. Ricard, F. Mathey, P. Le Floch, *Organometallics* **2001**, *20*, 3304.
- [33] G. M. Sheldrick, SHELXS-97, *Acta Crystallogr.* **1990**, *A46*, 467.
- [34] G. M. Sheldrick, SHELXL-97, University of Göttingen, **1997**.

Received: August 27, 2002 [F4372]